A Robotic, Dual-Sensing, Functional Optical Imaging System for Breast Cancer Detection

Rabah Al Abdi[1], Christoph H. Schmitz[2], Rehman Ansari[1,3], Randall Andronica[1], Yong Xu[1,3], Harry L. Graber[1,3], and Randall L. Barbour[1,3]

[1] SUNY Downstate Medical Center, USA; [2] NIRx Medizintechnik GmbH, Germany; [3] NIRx Medical Technologies LLC, USA

ABSTRACT

Simultaneous dual-breast diffuse optical tomography (DOT) using our first-generation imager design has been shown to achieve high diagnostic sensitivity and specificity (>95%). A new DOT system has been developed that supports examination of additional features of the tumor phenotype and their interactions. Improvements include ability to accommodate a wide range of breast sizes, measures in the seated position, and application of precise articulation maneuvers that document spatial variations in Young's modulus and concurrent hemodynamic responses. Preliminary clinical studies document that a wealth of discriminatory features can be identified that serve to explore functional differences between tumor and surrounding host tissues.

The system is described, and preliminary experimental results from combined optical/stress-strain measurements on a healthy and tumor-bearing breast are shown.

MOTIVATION

Our strategy for increasing diagnostic power of optical breast imaging:

- Imaging of hemodynamic activity of breast vasculature during rest allows identification of tissues with deranged autoregulation (e.g., cancerous and pre-cancerous states), with high contrast [1]
- Simultaneous dual-breast imaging allows for paired comparison between diseased and healthy tissue, thus increasing statistical robustness [2,3]
- Controllable pressure maneuvers with high precision increases the normal/tumor tissue contrast based on their hemodynamic response difference.[4] This is combined with the ability to re-distribute the blood in the breast by applying fine articulation.
- The stiffness of the breast tissue can be evaluated during the pressure maneuver. This increases the ability to differentiate breast cancer based on the fact that tumor tissue is stiffer than normal tissue. [5].
- The plastic deformation is an intrinsic property of biological tissue, and the characterization of the mechanical nature of tissue may serve as a diagnostic tool for breast cancer detection. [6]

Previously described instrumentation was used for method evaluation, and demonstrated the feasibility of the first two points listed above (1 and 2). Dual-breast imaging gives a potentially high diagnostic power for many uni-variate and multivariate diagnostic metrics based on bilateral dynamic contrasts in the resting state and Valsalva maneuver.

Some practical shortcomings also became clear, which were addressed in the new imager design:

- Patients were required to lie prone, which for many was uncomfortable, and which interfered with the proper performance of provocation protocols.
- fixed-size plastic cups as fiber-optic interface:
  - limited anatomical adaptability: good optical contact could be achieved only for a subset of breast sizes and shapes;
  - circular cross-section maximizes measuring distances in the coronal plane, thus decreasing the achievable signal-to-noise ratio.
- Fairly sparse optode arrangement of 31 sources (S) x 31 detectors (D) per breast. Rigid dual-cup probe holder accommodated only limited breast sizes, or only a portion of the breast.

To alleviate these shortcomings, the new instrument was designed with the following features:

- Cart-based design and probe holders on two articulated arms, for independent positioning of the fibers on each breast, to allow imaging the subject in a comfortable sitting position.
- Increased no. of channels: 32S x 64D per breast (total of 2 x 2048 Ch. x 2 Wavelengths @ 1.8Hz)
- Measuring head design: clamshell mechanism
  - allows mild compression for better transmission
  - accommodates large range of breast sizes
  - allows pressure modulation
  - high spatial sensing density
- Integrated strain gauges measure pressure reaction of tissue.
- Built-in stepper motors apply pressure maneuver with high precision.

INSTRUMENTATION

The instrument design (see Fig. 1) expands on proven technology described before [7]:

- **Detection**: 2x 64-channel detector modules with Si photodiodes, adaptive gain switching, and analog lock-in amplification for demodulation of two frequency-encoded wavelengths. Signal sampling by 4, 64-analog-channel data acquisition boards (National Instruments PCI 6033).
- **Probe holders (measuring head)**: A Clamshell design comprising mechanical fingers to arrange optodes in linear arrays of four (Fig. 1c) on the superior breast surface. The lower half of the device consists of an adjustable 4 element nested arc design that enable measurements within 1 cm of the chest wall. Verital distance between top and bottom fingers is variable, via a single adjustment screw, to accommodate different breast sizes. The upper half of the clamshell is formed by 8 cantilevered metal rods (Fig 1b,c) which can be adjusted to accommodate different breast sizes and to apply a controlled pressure to the tissue.
- **Strain gauges**: 8 semiconductor strain gauges (SS-090-060-500P by Micron Instruments, Inc., CA) are incorporated into each measuring head to monitor pressure exerted onto the breast tissue by sensing minute bending in the support rods, causing changes in resistance (Fig. 1d). Gauge resistance changes linearly with the force applied to the rod (5.7 Ω/N, linearily better than 1% over a range of 15N, see Fig. 1e). Nominal resting resistance of the devices: 540 Ω @ 25.5°C; load-free mounted resistance (offset) ~ 410 Ω. Individual gauge response vary by less than 10%. Gauges are read out with a voltage divider and sampled by a data acquisition board (USB 6218 by National Instruments Corp, TX). Achievable measurement sensitivity is 16 mN.
- **Linear stepper motor**: The two measuring heads of the breast imager are powered by sixteen linear stepper motors (42DBL10D2B-K by Portescap Inc. TX), so that each finger can be moved forward or backward to deform the breast with high accuracy (~1mm) and over a wide range (90 mm). By moving the finger toward the breast, a maximum force up to 7 N can be applied. Sixteen dual full-bridge drivers designed to accept standard TTL logic levels from a host computer are used to control movement and the speed of the stepper motors through a USB data acquisition card (USB-6118) from National Instrument, TX. A high speed closed-loop feedback (25 cycles per second), written in LabView software, between the strain gauge output and the stepper motor drivers allow changing of applied force to the surface of the breast with a maximum rate 1.8 N / sec.

Fig. 1: Instrumentation

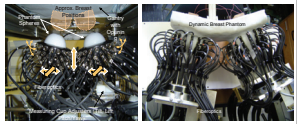

(a) Previous dual-breast interface (b) New dual-breast interface w/ dynamic phantom

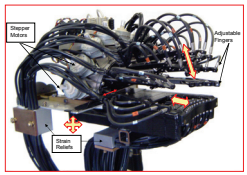

(c) Side view of measuring head

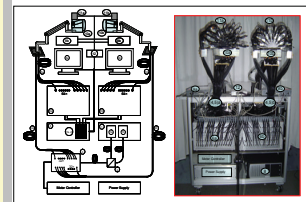

Figure 1, Imager components: 1- Laser controller, 1a,b- Laser driver 780 nm and 830 nm, 2- Wavelength combiner, 3- Optical switch, 4a,b- Illumination fibers for left and right, 5a,b- Detection fibers, 6 a,b- Optical detectors, 7a ,d- Data acquisition cards, 8- Personal computer, 9a,b- Displays, 9a,b- Stepper motor drivers, 10a,b- Measuring heads, 11 a,b- stepper motors, 12- USB Data Acquisition.

(d) Breast imager schematic diagram (e) Breast imager photograph.

Table 1: Breast imager performance and specification

Type	Parameter	Value
Optical	Wavelengths	760 nm and 830 nm
	Number of Sources	64 (32 left and 32 right)
	Number of detectors	128 (64 left and 64 right)
	Detector Sensitivity	10 pW
	Dynamic range	$1:10^9$ (180 dB)
	Cross-talk (D-MUX)	$< 1:10^{-5}$
	Cross-talk (detector channels)	$< 1:10^{-6}$
	Data acquisition rate	1.8 Hz x 8192 channels
Mechanical	Pressure sensitivity	0.04 N (0.01 lb)
	Capacity	15 N (3.4 lb)
	Cross-talk	$1: 10^{-2}$
	Repeatability (Std. Dev.)	0.08 N (0.02 lb)
	Fingers movement range	90 mm
	Data acquisition rate	25 Hz x 16 channels

Fig. 2 Schematic of physical measurements with the breast imager and their interpretation

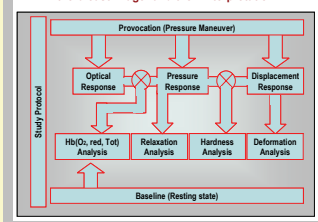

Fig. 3: Study responses

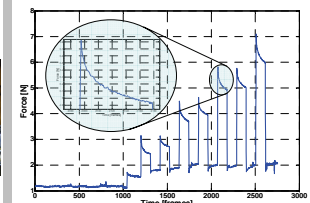

(a) Pressure response of finger (1)

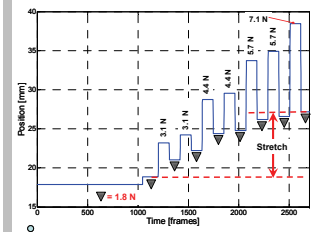

(b) Deformation of the breast under finger (1)

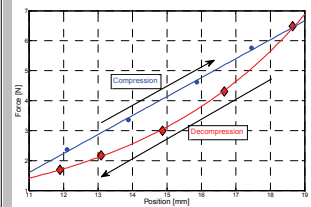

(c) Stress-strain relationship in the compression and decompression phases.

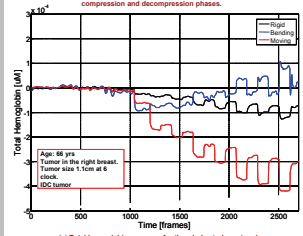

(c) Total hemoglobin response for the whole study protocol.

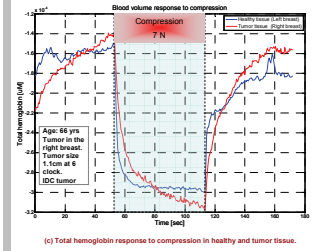

(c) Total hemoglobin response to compression in healthy and tumor tissue.

ACKNOWLEDGMENTS

We would like to acknowledge and thank Drs. Zaw Bo and Begum Noor for their help on this project.
This research was supported by the National Institutes of Health (NIH) under grants 1R43CA91725-1A1, R21-HL67387, R21-DK63692, and R41-CA96102; by the U.S. Army under grant DAMD17-03-C-0018; by the New York State Department of Health; and by the Susan G. Komen Foundation under grant IMG0403022.

Fig. 4: Schematic of different classes of responses

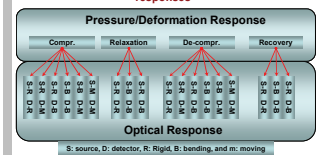

Fig. 5: Stretch Response.

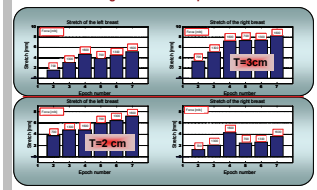

Fig. 6: Hardness (Stiffness) results.

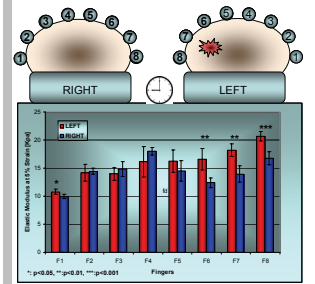

Fig. 7: Finite Element Mesh for image reconstruction

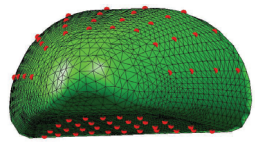

Fig. 8: 1st derivative response of Hbtot to applied pressure.

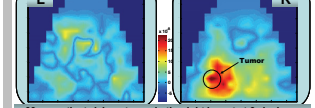

66 yrs patient, 1.1 cm tumor in the right breast at 6 clock

Fig. 9: Example of Image Recovery from Dynamic Phantom

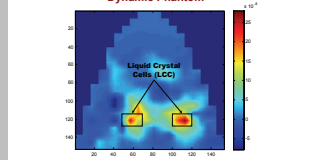

METHODS

- The study protocol got approved by the Institutional Review Board at State University of New York Downstate Medical Center (protocol # 04-216).
- Measurements were performed in the seated position. Each measuring head was adjusted to make comfortable contact with the breast. Following gross adjustments, fine adjustments in optode position were made under feedback control to a fixed applied pressure (usually 400 mlbs).
- After applying initial pressure (~0.4 lb/ 1.8 N), collection of optical data started with a resting-state measurement lasting approximately 10 minutes.
- A sequence of external pressure changes, of varying magnitudes (max 1.6 lb / 7 N) and 60-second duration, interspaced with 60-second resting intervals, are applied to both breasts simultaneously while the optical data is being collected (Fig 3).
- The study usually takes about 50 minutes and all the optical, pressure, and deformation are stored.
- Two host computers are used to control the breast imager using LabView software, one for optical signal collection and the other to control and record the movement of the fingers and their pressure reading.
- The applied pressure, the position of the fingers, and all the optical signal levels are displayed on real time on the screen.

RESULTS

- By deforming the breast to provoke the hemodynamic changes in the breast, six classes of the optical response occur simultaneously. Some of them are pure hemodynamic response and the others are dominated by a changing in the path length between the source-detector pairs (Fig 4).
- A temporary plastic deformation of the breast is seen to occur in response to application of several pressure pulse maneuvers causing the breast not to return to its original shape. Tumor bearing breasts exhibit a consistently greater plastic deformation than normal breast under the same conditions (Fig 5).
- Estimates of tissue stiffness are determined from the 1st derivative of the strain-stress response. Fig 6 shows that the finger closest to the tumor senses a stiffer response than those at greater distances from the tumor.
- A Finite Element Mesh (FEM) corresponding to the shape of a supported breast was developed for image reconstruction (Fig. 7).
- Optical data is preprocessed (normalized and filtered, etc), and using the normalized difference method, 3D images of oxy-, deoxy-, and total hemoglobin are generated.
- Measures of amplitude and its variability across the temporal and spatial dimensions are used to diagnose presence of tumors based on the imbalance of its oxygen demand and supply [8].
- The slope of the hemodynamic response (e.g. Hb-total) in the compression phase is also used for tumor detection based on their sluggish hemodynamic response to compression (larger slope) (Fig 8).
- Phantom measurements demonstrate (1) accurate inclusion localization and (2) highly linear relation between programmed and reconstructed inclusion optical density. [9] Fig. 9 shows a 3D image obtained from an experiment on the breast phantom.

SUMMARY

- The described breast imager is capable to sense physiological changes in the breast cancer from three independent physical measurements, optical (hemodynamic), deformation, and elasticity.
- Monitoring the hemodynamic response of the breast in compression, relaxation, decompression, and recovery phases produce many uni-variate and multivariate diagnostic metrics based on bilateral dynamic contrasts in the compression phases.
- The tumor bearing breast is stiffer than the unaffected contralateral breast, and the breast imager is able to evaluate this difference in stiffness.
- The breast responds with a temporary plastic deformation when several epochs of compression are applied within short period of time (~ 10min), and this plasticity increase when in the presence of tumor.
- Phantom studies support the ability of the breast imager to localize any hemodynamic response in the breast.

REFERENCES

[1] R.L. Barbour, H.L. Graber, Y. Pei, S. Zhong, C.H. Schmitz, "Optical tomographic imaging of dynamic features of dense-scattering media," JOSA A 18, 3018-3036 (2001).

[2] C.H. Schmitz, D.P. Klemer, R.E. Hardin, M.S. Katz, Y. Pei, H.L. Graber, M.B. Levin, R.D. Levina, N.A. Franco, W.B. Solomon, R.L. Barbour, "Design and implementation of dynamic near-infrared optical tomographic imaging instrumentation for simultaneous dual-breast measurements," Applied Optics 44, 2140-2153 (2005).

[3] Y. Pei, H.L. Graber, M. Farber, C.H. Schmitz, Y. Xu, P. Toubas, N. Patel, M.S. Katz, W.B. Solomon, and R.L. Barbour, "Tumor detection by simultaneous bilateral diffuse optical tomography (DOT) breast imaging," Poster No. B2 at Fifth Inter-Institute Workshop on Optical Diagnostic Imaging from Bench to Bedside at the National Institutes of Health (Bethesda, MD, September 25-27, 2006).

[4] S. Carp, J. Selb, Q. Fang, R. Moore, D. Kopans, E. Rafferty, and D. Boas, "Dynamic functional and mechanical response of breast tissue to compression", Optics Express, Vol. 16, Issue 20, pp. 16064-16078, (2008).

[5] P. Wellman, R. Howe, E. Dalton, and K. Kern, "Breast Tissue Stiffness in Compression is Correlated to Histological Diagnosis", Ultrason Imaging. (2008). http://biorobotics.harvard.edu/pubs/mechprops.pdf

[6] C. Williams, B. Clymer, P. Schmalbrock, "Biomechanics of Breast Tissue: Preliminary study of shape deformation of normal breast tissue." Abstract. 6th Annual Meeting of the International Society for Magnetic Resonance in Medicine. Sydney, Australia.

[7] C.H. Schmitz, M. Löcker, J.M. Lasker, A.H. Hielscher, R. L. Barbour, "Instrumentation for fast functional optical tomography," Review of Scientific Instruments, Vol. 73, pp. 429-439 (2002).

[8] H. L. Graber, Y. Pei, Y. Xu, M. Farber, M. S. Katz, N. Patel, W. B. Solomon, D. C. Lee, R. L. Barbour, "Utility of Spontaneous and Evoked Vascular Dynamics, Assessed by Near Infrared Diffuse Optical Tomography, for Diagnosis of Breast Cancer", Applied Optics (submitted).

[9] R.L. Barbour, R. Ansari, R. Al abdi, H.L. Graber, M.B. Levin, Y. Pei, C.H. Schmitz, and Y. Xu, "Validation of near infrared spectroscopic (NIRS) imaging using programmable phantoms," Paper 687002 in Design and Performance Validation of Phantoms Used in Conjunction with Optical Measurements of Tissue (Proceedings of SPIE, Vol. 6870), R.J. Nordstrom, Ed. (2008). Copyright Society of Photo-Optical Instrumentation Engineers.